2021 60th IEEE Conference on Decision and Control (CDC)
December 13-15, 2021. Austin, Texas

Heterogeneous Formation Control: a Bearing Rigidity Approach

Beniamino Pozzan, Giulia Michieletto, Angelo Cenedese and Daniel Zelazo

2021 60th IEEE Conference on Decision and Control (CDC) | 978-1-6654-3659-5/21/$31.00 ©2021 IEEE | DOI: 10.1109/CDC45484.2021.9683374

***Abstract*— This work proposes a formation control law for multi-agent systems whose components are heterogeneous in terms of actuation capabilities, but at the same time are all able to retrieve bearing information w.r.t. some neighbors in the group. The designed controller exploits the results of the bearing rigidity theory deriving from the modeling of heterogeneous formations as *generalized frameworks*. The outlined solution is compared with a leader-follower combination of existing rigidity based homogeneous formation controllers in order to highlight the easy tuning, the flexibility w.r.t. the formation composition, and the increased efficiency of the new proposed control approach. A sufficient condition ensuring the convergence of the designed controller is also given.**

I. Introduction

In a broad sense, bearing rigidity theory aims at investigating the stiffness properties of given multi-element systems whose components are mutually constrained in terms of relative orientation [1]. In the last years, the study of such a theory has been deeply encouraged by the emergence of multi-agent systems as an enabling paradigm in several contexts. The bearing rigidity framework, indeed, suitably fits for applications related to the estimation and control of mobile agent formations wherein the involved devices are aware of their orientation w.r.t. some neighbors in the group. In this perspective, bearing constraints are virtual and the rigidity property of the multi-element system relies on the preservation of the agent interactions [2].

One of the aims of the bearing rigidity theory is the identification of the conditions under which the geometric pattern induced by a set of points in any metric space can be uniquely determined by the bearing vectors between these points [3]. Hence, bearing rigidity notions can be exploited in the design of multi-agent formation control laws, especially by accounting for the system rigidity as an architectural requirement for the convergence of the agents to a desired spatial configuration. Thus, recently, several bearing rigid based formation stabilization approaches have been proposed for multi-agent systems modeled as frameworks embedded in $SE(2)$, $SE(3)$, and more generic smooth manifolds [4]–[7]. Most of the existing strategies apply to homogeneous formations, intended for groups of agents characterized by the same actuation capabilities. For instance, in [8], a distributed bearing-only formation control strategy is outlined for a team of unmanned ground vehicles (UGVs), ensuring the global asymptotic stability when the agents sensing interplay is minimal to guarantee the bearing preservation only in case of translations and scaling of the whole multi-robot system. Similarly, in [9], a decentralized formation controller is designed and tested on a group of quadrotors aiming at steering the team of unmanned aerial vehicles (UAVs) towards a formation defined in terms of desired bearings.

Motivated, instead, by the IoT perspective, encouraging also the cooperation among devices with various actuation capabilities, this work focuses on *heterogeneous* formations, meant as multi-element systems whose components have different degrees of freedom (dofs) as to controllable variables. Assuming all the involved agents to be characterized by (local) communication and bearing sensing capabilities, the given contribution consists in the design of a distributed control law to stabilize a group of heterogeneous agents by preserving the existing bearing measurements. In doing this, the heterogeneous formations are modeled as *generalized* frameworks, namely frameworks embedded in the differential manifold $\mathbb{R}^3 \times \mathbb{S}^3$ which allows to describe the pose (position and orientation) of a rigid body in the 3D space by adopting the quaternion formalism [4], enriched with a mathematical codification of the agents actuation capabilities. The effectiveness of the proposed controller is confirmed by both rigorous proof of convergence and numerical results of an extensive simulations campaign. In particular, accounting for a formation involving (fully actuated) aerial and ground vehicles, the outlined solution is compared with an ad-hoc designed leader-follower combination of the bearing rigidity based controllers in [4] and [8] for the stabilization of planar and (fully-actuated) aerial multi-agents systems, respectively.

The rest of the work is organized as follows. Sec. II is devoted to the modeling of the heterogeneous formations. The proposed distributed control solution is described in Sec. III and its effectiveness is discussed in Sec. IV. Sec. V summarize the principal strengths of the proposed approach and Sec. VI draws the main conclusions.

II. Heterogeneous Formation Characterization

This section provides a mathematical model for a heterogeneous formation composed of $n \geq 3$ agents (with some dofs) able to acquire bearing measurements w.r.t. its neighbors in the group and to communicate with them.

A. Single Agent Model

Each i-th agent, $i \in \{1 \dots n\}$, in a heterogeneous formation can be modeled as a rigid body acting in 3D space. Thus,

This work was partly supported by MIUR (Italian Ministry for Education) under the initiative "Departments of Excellence" (Law 232/2016) and by University of Padova under the Visiting Scientist 2019 program and the TSTARK DEI-SEED 2020 project.

B. Pozzan and A. Cenedese are with the Department of Information Engineering, G. Michieletto is with the Department of Engineering and Management, both at the University of Padova, Padova, Italy; D. Zelazo is with the Faculty of Aerospace Engineering, Technion-Israel Institute of Technology, Haifa, Israel. Corresponding author: B. Pozzan (beniamino.pozzan@phd.unipd.it).

its spatial displacement can be characterized by introducing the local frame $\mathcal{F}_i$ (*body frame*), having origin O_i coincident with the agent center of mass and axes identified by the unit vectors $\{\mathbf{e}_1, \mathbf{e}_2, \mathbf{e}_3\}$ defining the canonical basis of $\mathbb{R}^3$, and the inertial frame $\mathcal{F}_W$ (*world frame*), fixed and common, even if unknown, for all the formation components. Indeed, given the vector $\mathbf{p}_i \in \mathbb{R}^3$ of the coordinates of O_i in $\mathcal{F}_W$ and the unit quaternion $\mathbf{q}_i = [\eta_i \;\; \boldsymbol{\varepsilon}_i^\top]^\top \in \mathbb{S}^3$ defining the rotation of $\mathcal{F}_i$ w.r.t. $\mathcal{F}_W$, the vector $\mathbf{x}_i = [\mathbf{p}_i^\top \;\; \mathbf{q}_i^\top]^\top$ belonging to the differential manifold $\mathbb{R}^3 \times \mathbb{S}^3$ identifies the i-th agent pose in world frame, i.e., its time-varying *configuration*.

Introducing the linear velocity $\mathbf{v}_i \in \mathcal{V}_i \subseteq \mathbb{R}^3$ of O_i w.r.t. $\mathcal{F}_W$ and the angular velocity $\boldsymbol{\omega}_i \in \Omega_i \subseteq \mathbb{R}^3$ of $\mathcal{F}_i$ w.r.t. $\mathcal{F}_W$, both in body frame, the i-th agent kinematics is governed by

$$\dot{\mathbf{p}}_i = \mathbf{R}_i \mathbf{v}_i, \qquad \dot{\mathbf{q}}_i = \frac{1}{2}\mathbf{M}(\mathbf{q}_i)\boldsymbol{\omega}_i, \tag{1}$$

where $\mathbf{R}_i \in SO(3)$ is the rotation matrix associated to $\mathbf{q}_i$ and the matrix $\mathbf{M}(\mathbf{q}_i) \in \mathbb{R}^{4\times 3}$ maps the agent angular velocity into the time derivative of its quaternion based orientation.

The linear and angular velocity in (1) can be interpreted as the controllable variables of the i-th agent. When $\mathcal{V}_i = \Omega_i = \mathbb{R}^3$, the agent is *fully*-actuated: it can translate and rotate in any direction of the 3D space having three translational and three rotational controllable degrees of freedom (cdfos). When $\mathcal{V}_i$ or $\Omega_i \subset \mathbb{R}^3$, instead, the agent is *under*-actuated and its movement is constrained only in some directions, having less than 6 cdofs. Indicating with $c_i \in \{0 \dots 6\}$ the i-th agent cdofs, it is suitable to introduce the *i-th agent commands vector* $\boldsymbol{\delta}_i$ belonging to the *i-th agent instantaneous variation domain* $\mathcal{I}_i \subseteq \mathbb{R}^{c_i}$, which specifies the agent actuation capabilities through the *selection* map

$$S_i \colon \mathcal{I}_i \to \mathcal{V}_i \times \Omega_i, \quad \boldsymbol{\delta}_i \mapsto \begin{bmatrix}\mathbf{v}_i^\top & \boldsymbol{\omega}_i^\top\end{bmatrix}^\top. \tag{2}$$

Hereafter the following *decoupling* hypothesis is assumed in regard to the agent translation and rotation movements, nonetheless the control law described in Sec. III is valid also when this is not in place, with minor suitable changes.

Assumption II.1. Any i-th agent can provide decoupled translation and rotation commands, meaning that $\boldsymbol{\delta}_i$ in (2) is made up of two components that can be independently assigned. Formally, $\boldsymbol{\delta}_i = [\boldsymbol{\delta}_{p,i}^\top, \boldsymbol{\delta}_{o,i}^\top]^\top \in \mathcal{I}_i = \mathcal{I}_{p,i} \times \mathcal{I}_{o,i}$ with $\boldsymbol{\delta}_{p,i}$ and $\boldsymbol{\delta}_{o,i}$, respectively associated to the agent linear and angular velocity, $\mathcal{I}_{p,i}$ and $\mathcal{I}_{o,i}$ representing the *i-th agent instantaneous position* and *orientation variation domains*.

Under Ass. II.1, the i-th agent total number of cdofs results $c_i = c_{t,i} + c_{r,i}$ with $c_{t,i} = \dim(\mathcal{I}_{p,i}) = \dim(\mathcal{V}_i)$ and $c_{r,i} = \dim(\mathcal{I}_{o,i}) = \dim(\Omega_i)$ denoting its translational and rotational cdofs, respectively. Moreover, the *selection* map S_i in (2) can be split into the following terms,

$$S_{p,i} \colon \mathcal{I}_{p,i} \to \mathcal{V}_i, \quad \boldsymbol{\delta}_{p,i} \mapsto \mathbf{v}_i \tag{3a}$$
$$S_{o,i} \colon \mathcal{I}_{o,i} \to \Omega_i, \quad \boldsymbol{\delta}_{o,i} \mapsto \boldsymbol{\omega}_i, \tag{3b}$$

with bijective $S_{p,i}$. In addition, accounting for real-world scenarios, hereafter, the structure of the maps $S_{p,i}, S_{o,i}$ is assumed as follows.

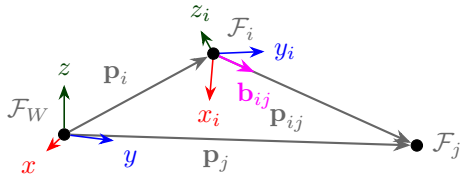

Fig. 1: agents sensing interaction - magenta arrow indicates the bearing measurement of i-th agent w.r.t. its j-th neighbor.

Assumption II.2. The maps $S_{p,i}, S_{o,i}$ are linear, hence it is

$$\mathbf{v}_i = S_{p,i}(\boldsymbol{\delta}_{p,i}) = \mathbf{S}_{p,i}\boldsymbol{\delta}_{p,i} \qquad \mathbf{S}_{p,i} \in \mathbb{R}^{3\times c_{p,i}}, \tag{4a}$$
$$\boldsymbol{\omega}_i = S_{o,i}(\boldsymbol{\delta}_{o,i}) = \mathbf{S}_{o,i}\boldsymbol{\delta}_{o,i} \qquad \mathbf{S}_{o,i} \in \mathbb{R}^{3\times c_{o,i}}. \tag{4b}$$

The next example aims at clarifing the introduced model.

Example II.1. For a UGV that can can rotate only around the z-axis of its body frame and translate on the (xy)-plane, we have $\mathcal{V}_i = \text{span}\{\mathbf{e}_1, \mathbf{e}_2\}$ and $\Omega_i = \text{span}\{\mathbf{e}_3\}$, and thus $\mathcal{I}_{p,i} = \mathbb{R}^2$, $\mathcal{I}_{o,i} = \mathbb{R}$, $\mathbf{S}_{p,i} = [\mathbf{e}_1 \;\; \mathbf{e}_2]$, and $\mathbf{S}_{o,i} = \mathbf{e}_3$.

In this work, each agent is also assumed to be able to gather bearing measurements w.r.t. some neighbors in the group. Specifically, the *bearing measurement* recorded by the i-th agent w.r.t. the j-th neighbor is supposed to be acquired in $\mathcal{F}_i$, however it can be expressed in terms of position and orientation of the involved agents in $\mathcal{F}_W$ as follows

$$\mathbf{b}_{ij} = \mathbf{R}_i^\top \bar{\mathbf{p}}_{ij} \in \mathbb{S}^2, \quad \bar{\mathbf{p}}_{ij} = \frac{\mathbf{p}_j - \mathbf{p}_i}{\|\mathbf{p}_j - \mathbf{p}_i\|} \in \mathbb{S}^2. \tag{5}$$

A graphical representation of the vector $\mathbf{b}_{ij}$ is given in Fig. 1.

Finally, each agent is also supposed to communicate with its neighbors. In particular, it can share the retrived measurements, allowing the sensed formation components to estimate their relative orientation (see Appendix).

B. Networked System Model

Being a networked architecture, any formation can be modeled according to the graph-based multi-agent system representation. In particular, a heterogeneous formation made up of n-agents fulfilling the assumptions of Sec. II-A can be associated to a *directed graph* $\mathcal{G} = (\mathcal{V}, \mathcal{E})$ where the node $v_i \in \mathcal{V}$ corresponds to the i-th agent, $i \in \{1 \dots n\}$, and the directed edge $e_k = e_{ij} = (v_i, v_j) \in \mathcal{E}$ indicates that the i-th agent can measure the bearing w.r.t. j-th agent and communicate with it. Note that agent sensing is not assumed to be bidirectional: $(v_i, v_j) \in \mathcal{E}$ does not imply $(v_j, v_i) \in \mathcal{E}$.

Stacking the position and orientation of all the formation components into the vectors $\mathbf{p} = [\mathbf{p}_1^\top \dots \mathbf{p}_n^\top]^\top \in \mathbb{R}^{3n}$ and $\mathbf{q} = [\mathbf{q}_1^\top \dots \mathbf{q}_n^\top]^\top \in \mathbb{S}^{3^n}$, respectively, the time-varying *configuration of the whole system* is, thus, represented by $\mathbf{x} = [\mathbf{p}^\top \;\; \mathbf{q}^\top]^\top \in \mathbb{R}^{3n} \times \mathbb{S}^{3^n}$. Furthermore, introducing the vector $\mathbf{u} = [\mathbf{v}_1^\top \dots \mathbf{v}_n^\top, \boldsymbol{\omega}_1^\top \dots \boldsymbol{\omega}_n^\top]^\top \in \prod_{i=1}^n \mathcal{V}_i \times \prod_{i=1}^n \Omega_i$ and accounting for (1), the evolution of the formation is governed by

$$\dot{\mathbf{x}} = \begin{bmatrix}\mathbf{D}_1(\mathbf{q}) & \mathbf{0}_{3n\times 3n} \\ \mathbf{0}_{4n\times 3n} & \mathbf{D}_2(\mathbf{q})\end{bmatrix}\mathbf{u} = \mathbf{D}(\mathbf{q})\mathbf{u}, \tag{6}$$

$$\begin{cases} \begin{bmatrix} \mathbf{0}_{3\times3(i-1)} & -\check{d}_{ij}\mathbf{P}(\mathbf{b}_{ij})\mathbf{S}_{p,i} & \mathbf{0}_{3\times3(j-i-1)} & \check{d}_{ij}\mathbf{P}(\mathbf{b}_{ij})\mathbf{R}_i^\top\mathbf{R}_j\mathbf{S}_{p,j} & \mathbf{0}_{3\times3(n-j+i-1)} & [\mathbf{b}_{ij}]_\times\mathbf{S}_{o,i} & \mathbf{0}_{3\times3(n-i)} \end{bmatrix} & \text{if } i<j, \\ \begin{bmatrix} \mathbf{0}_{3\times3(j-1)} & \check{d}_{ij}\mathbf{P}(\mathbf{b}_{ij})\mathbf{R}_i^\top\mathbf{R}_j\mathbf{S}_{p,j} & \mathbf{0}_{3\times3(i-j-1)} & -\check{d}_{ij}\mathbf{P}(\mathbf{b}_{ij})\mathbf{S}_{p,i} & \mathbf{0}_{3\times3(n-1)} & [\mathbf{b}_{ij}]_\times\mathbf{S}_{o,i} & \mathbf{0}_{3\times3(n-i)} \end{bmatrix} & \text{if } j>i, \end{cases} \tag{9}$$

where $\mathbf{D}_1(\mathbf{q}) = \mathrm{diag}(\mathbf{R}_i) \in \mathbb{R}^{3n\times3n}$ and $\mathbf{D}_2(\mathbf{q}) = \mathrm{diag}(\frac{1}{2}\mathbf{M}(\mathbf{q}_i)) \in \mathbb{R}^{4n\times3n}$ are diagonal block matrices. In detail, under Ass. II.2, the relation (6) can be rewritten introducing the *commands vector* $\boldsymbol{\delta} = [\boldsymbol{\delta}_{p,1}^\top \dots \boldsymbol{\delta}_{p,n}^\top \boldsymbol{\delta}_{o,1}^\top \dots \boldsymbol{\delta}_{o,n}^\top]^\top$ belonging to the *instantaneous variation domain* $\mathcal{I} = \prod_{i=1}^n \mathcal{I}_{p,i} \times \prod_{i=1}^n \mathcal{I}_{o,i}$ having dimension $c = c_t + c_r$ with $c_t = \sum_{i=1}^n c_{t,i}$ and $c_r = \sum_{i=1}^n c_{r,i}$. It holds that

$$\dot{\mathbf{x}} = \mathbf{D}(\mathbf{q}) \begin{bmatrix} \mathbf{S}_p & \mathbf{0} \\ \mathbf{0} & \mathbf{S}_o \end{bmatrix} \boldsymbol{\delta} = \mathbf{D}(\mathbf{q})\mathbf{S}\boldsymbol{\delta}, \tag{7}$$

with $\mathbf{S}_p = \mathrm{diag}\left(\mathbf{S}_{p,i}\right) \in \mathbb{R}^{3n\times c_t}$, $\mathbf{S}_o = \mathrm{diag}\left(\mathbf{S}_{o,i}\right) \in \mathbb{R}^{3n\times c_o}$.

Given these premises, any heterogeneous formation can be modeled as a *generalized framework* whose dynamic behavior is described by (7).

Definition II.1 (Generalized Framework)**.** A *generalized framework* is an ordered triple $(\mathcal{G}, \mathbf{x}, \mathcal{H})$ consisting of a connected graph $\mathcal{G} = (\mathcal{V}, \mathcal{E})$ with $|\mathcal{V}| = n \geq 3$ and $|\mathcal{E}| = m$, a configuration $\mathbf{x} \in \mathbb{R}^{3n} \times \mathbb{S}^{3^n}$, and a collection of instantaneous variation domains $\mathcal{H} = \{\mathcal{I}_1 \dots \mathcal{I}_n\}$.

According to most of the rigidity literature, the graph $\mathcal{G}$ modeling the formation is hereafter assumed to be fixed over time: the agents can modify their pose in $\mathcal{F}_W$ but they preserve the interaction w.r.t. their neighbors. In this scenario, the information on the available measurements can be summarized through the introduction of the following *bearing function*, which turns then out to be useful also to identify the *formation shape* in terms of the bearings among all the pairs of agents, represented by the directed complete graph $\mathcal{K}$ associated to $\mathcal{G}$.

Definition II.2 (Bearing Function)**.** Given a formation modeled as a generalized framework $(\mathcal{G}, \mathbf{x}, \mathcal{H})$, the *bearing function* is the map associating the configuration $\mathbf{x} \in \mathbb{R}^{3n} \times \mathbb{S}^{3^n}$ to the vector $\mathbf{b}_\mathcal{G}(\mathbf{x}) = [\mathbf{b}_1^\top \dots \mathbf{b}_m^\top]^\top \in \mathbb{S}^{2^m}$ stacking all the available bearing measurements.

Definition II.3 (Formation shape)**.** Given a formation modeled as a generalized framework $(\mathcal{G}, \mathbf{x}, \mathcal{H})$, its shape is characterized by the collection of *all* the possible bearing measurements, namely, by the vector $\mathbf{b}_\mathcal{K}(\mathbf{x}) \in \mathbb{S}^{2^{n(n-1)}}$ where $\mathcal{K}$ is the complete graph associated to $\mathcal{G}$.

III. Bearing Rigidity Based Formation Control

The main contribution of this work consists in the design of a distributed controller aiming at stabilizing any heterogeneous formation undergoing the characterization of Sec. II through the solution of the following problem.

Problem III.1 ((Bearing Based) Formation Stabilization)**.** For a given heterogeneous formation modeled as a generalized framework subject to (7), consider a desired formation shape described by $\mathbf{b}_\mathcal{K}^* \in \mathbb{S}^{2^{n(n-1)}}$ which is *feasible* meaning that it exists a configuration $\mathbf{x}^*$ such that $\mathbf{b}_\mathcal{K}^* = \mathbf{b}_\mathcal{K}(\mathbf{x}^*)$. The *(bearing based) formation stabilization problem* consists in asymptotically zeroing the *shape error* $\boldsymbol{e}_\mathcal{K}(\mathbf{x}) \in \mathbb{R}^{3n(n-1)}$ defined as

$$\boldsymbol{e}_\mathcal{K}(\mathbf{x}) = \mathbf{b}_\mathcal{K}(\mathbf{x}) - \mathbf{b}_\mathcal{K}^*. \tag{8}$$

Prob. III.1 is here faced resting on the main notions of the bearing rigidity theory, applied to heterogeneous formations.

A. Preliminaries on Bearing Rigidity Theory

As for the homogeneous case, the *bearing rigidity matrix* associated to a heterogeneous multi-agent system describes the relation between the command vector and the time derivative of the bearing measurements vector.

Definition III.1 (Bearing Rigidity Matrix)**.** Given a formation modeled as a generalized framework $(\mathcal{G}, \mathbf{x}, \mathcal{H})$, the *bearing rigidity matrix* is the matrix $\mathbf{B}_\mathcal{G}(\mathbf{x}) \in \mathbb{R}^{3m\times c}$ that satisfies the relation $\dot{\mathbf{b}}_\mathcal{G}(\mathbf{x}) = \mathbf{B}_\mathcal{G}(\mathbf{x})\boldsymbol{\delta}$.

Note that, based on (4), the expression of the k-th row block of $\mathbf{B}_\mathcal{G}(\mathbf{x})$ results as in (9). Moreover, the computation of such a matrix allows to investigate the configuration variations that affect the formation shape, i.e., the generally called formation *infinitesimal bearing rigidity property*.

Definition III.2 (Infinitesimal Bearing Rigidity)**.** A formation modeled as a generalized framework $(\mathcal{G}, \mathbf{x}, \mathcal{H})$ is said to be *infinitesimal bearing rigid* (IBR) if $\ker\left(\mathbf{B}_\mathcal{K}(\mathbf{x})\right) = \ker\left(\mathbf{B}_\mathcal{G}(\mathbf{x})\right)$, where $\mathbf{B}_\mathcal{K}(\mathbf{x})$ is the bearing rigidity matrix associated to the complete graph $\mathcal{K}$.

B. Stabilization Control Law

Inspired by [2], [4], [8], [9], the bearing rigidity matrix is here exploited in the solution of Prob.III.1. Indeed, accounting for the *bearing error* $\mathbf{e}_\mathcal{G}(\mathbf{x}) \in \mathbb{R}^{3m}$ as

$$\mathbf{e}_\mathcal{G}(\mathbf{x}) = \mathbf{b}_\mathcal{G}(\mathbf{x}) - \mathbf{b}_\mathcal{G}(\mathbf{x}^*) = \mathbf{b}_\mathcal{G}(\mathbf{x}) - \mathbf{b}_\mathcal{G}^*, \tag{10}$$

it is possible to prove that its dynamics $\dot{\mathbf{e}}_\mathcal{G}(\mathbf{x}) = \dot{\mathbf{b}}_\mathcal{G}(\mathbf{x}) = \mathbf{B}_\mathcal{G}(\mathbf{x})\boldsymbol{\delta}$ asymptotically converges to zero by selecting the command vector as follows with $k_c > 0$ be a tunable gain

$$\boldsymbol{\delta} = k_c\mathbf{B}_\mathcal{G}^\top(\mathbf{x})\mathbf{b}_\mathcal{G}^*. \tag{11}$$

Proposition III.1. *Given a generalized framework $(\mathcal{G}, \mathbf{x}, \mathcal{H})$ subject to* (7)*, and a feasible bearing measurements vector $\mathbf{b}_\mathcal{G}^* \in \mathbb{S}^{2^m}$, it holds that $\mathbf{e}_\mathcal{G}(\mathbf{x}) = \mathbf{0}_{3m}$ is an asymptotically stable equilibrium point for the dynamics of the bearing error* (10) *driven by the control law* (11)*, namely for the system $\dot{\mathbf{e}}_\mathcal{G}(\mathbf{x}) = -k_c\mathbf{B}_\mathcal{G}(\mathbf{x})\mathbf{B}_\mathcal{G}^\top(\mathbf{x})\mathbf{e}_\mathcal{G}(\mathbf{x})$.*

Proof. Let consider the positive definite Lyapunov function

$$\mathrm{V}(\mathbf{e}_\mathcal{G}(\mathbf{x})) = \frac{1}{2k_c}\mathbf{e}_\mathcal{G}(\mathbf{x})^\top\mathbf{e}_\mathcal{G}(\mathbf{x}), \tag{12}$$

whose derivative $\dot{\mathrm{V}}(\mathbf{e}_\mathcal{G}(\mathbf{x})) = -\mathbf{e}_\mathcal{G}(\mathbf{x})^\top\mathbf{B}_\mathcal{G}(\mathbf{x})\mathbf{B}_\mathcal{G}^\top(\mathbf{x})\mathbf{e}_\mathcal{G}(\mathbf{x})$ is negative semi-definite since the product $\mathbf{B}_\mathcal{G}(\mathbf{x})\mathbf{B}_\mathcal{G}^\top(\mathbf{x})$ is

a positive semi-definite matrix for any $\mathbf{x} \in \mathbb{R}^{3n} \times \mathbb{S}^{3^n}$. It follows that $\mathbf{e}_{\mathcal{G}}(\mathbf{x}) = \mathbf{0}_{3m}$ is a simple stable equilibrium point for the bearing error dynamics, which converges to the set $\mathcal{Z} = \{\mathbf{e}_{\mathcal{G}}(\mathbf{x}) \mid \mathbf{x} \in \mathcal{U}(\mathbf{x}^*), \dot{\mathrm{V}}(\mathbf{e}_{\mathcal{G}}(\mathbf{x})) = 0\}$, where $\mathcal{U}(\mathbf{x}^*)$ is a neighborhood of $\mathbf{x}^*$. Now, exploiting the properties of the adjoint operator, the definition (10) and the fact that $\mathbf{B}_{\mathcal{G}}^{\top}(\mathbf{x})\mathbf{b}_{\mathcal{G}}(\mathbf{x}) = \mathbf{0}_c$ due to (9), one can realize that the equilibrium condition $\dot{\mathrm{V}}(\mathbf{e}_{\mathcal{G}}(\mathbf{x})) = 0$ implies that $\mathbf{B}_{\mathcal{G}}^{\top}(\mathbf{x})\mathbf{b}_{\mathcal{G}}(\mathbf{x}^*) = \mathbf{0}_c$. Then, accounting for the Taylor's expansion given $\mathbf{x}^* = \mathbf{x} + d\mathbf{x}$, it follows that

$$\begin{aligned}\mathbf{B}_{\mathcal{G}}^{\top}(\mathbf{x})\mathbf{b}_{\mathcal{G}}(\mathbf{x}+d\mathbf{x}) &\simeq \mathbf{B}_{\mathcal{G}}^{\top}(\mathbf{x})\big(\mathbf{b}_{\mathcal{G}}(\mathbf{x}) + \nabla_{\mathbf{x}}\mathbf{b}_{\mathcal{G}}(\mathbf{x})d\mathbf{x}\big),\\ &= \mathbf{B}_{\mathcal{G}}^{\top}(\mathbf{x})\nabla_{\mathbf{x}}\mathbf{b}_{\mathcal{G}}(\mathbf{x})d\mathbf{x}. \end{aligned} \tag{13}$$

Hence, according to (7), there exists $\boldsymbol{\delta} \in \bar{\mathcal{I}}$ such that

$$\mathbf{B}_{\mathcal{G}}^{\top}(\mathbf{x})\mathbf{e}_{\mathcal{G}}(\mathbf{x}) \simeq -\mathbf{B}_{\mathcal{G}}^{\top}(\mathbf{x})^{\top}\nabla_{\mathbf{x}}\mathbf{b}_{\mathcal{G}}(\mathbf{x})\mathbf{D}(\mathbf{q})\mathbf{S}\boldsymbol{\delta}. \tag{14}$$

On the other hand, exploiting the chain rule, the relation (7) and the bearing matrix definition, one can observe that

$$\nabla_{\mathbf{x}}\mathbf{b}_{\mathcal{G}}(\mathbf{x})\mathbf{D}(\mathbf{q})\mathbf{S} = \mathbf{B}_{\mathcal{G}}(\mathbf{x}), \tag{15}$$

leading to the conclusion that the condition $\dot{\mathrm{V}}(\mathbf{e}_{\mathcal{G}}(\mathbf{x})) = 0$ implies $\mathbf{B}_{\mathcal{G}}^{\top}(\mathbf{x})\mathbf{B}_{\mathcal{G}}(\mathbf{x})\boldsymbol{\delta} = \mathbf{0}_c$. In the light of this fact, given that $\ker(\mathbf{B}_{\mathcal{G}}^{\top}(\mathbf{x})\mathbf{B}_{\mathcal{G}}(\mathbf{x})) = \ker(\mathbf{B}_{\mathcal{G}}(\mathbf{x}))$, the elements in the set $\mathcal{Z}$ are associated to $\boldsymbol{\delta} \in \ker(\mathbf{B}_{\mathcal{G}}(\mathbf{x}))$. Hence, $\mathbf{e}_{\mathcal{G}}(\mathbf{x}) = \mathbf{b}_{\mathcal{G}}(\mathbf{x}) - \big(\mathbf{b}_{\mathcal{G}}(\mathbf{x}) + \mathbf{B}_{\mathcal{G}}(\mathbf{x})\boldsymbol{\delta}\big) = \mathbf{0}_{3m}$ belongs to $\mathcal{Z}$. □

Given these premises, it is then possible to prove that the infinitesimal rigidity property introduced in Def. III.2 is a sufficient condition for the solution of Prob. III.1.

Proposition III.2. *Consider a desired formation shape defined by $\mathbf{b}_{\mathcal{K}}^* \in \mathbb{S}^{2^{n(n-1)}}$. For any IBR generalized framework $(\mathcal{G}, \mathbf{x}, \mathcal{H})$ whose corresponding configuration $\mathbf{x}$ is in the neighborhood $\mathcal{U}(\mathbf{x}^*)$ of $\mathbf{x}^*$ such that $\mathbf{b}_{\mathcal{K}}^* = \mathbf{b}_{\mathcal{K}}(\mathbf{x}^*)$, the control law* (11) *solves the formation stabilization problem.*

Proof. For any IBR generalized framework $(\mathcal{G}, \mathbf{x}, \mathcal{H})$ with $\mathbf{x} \in \mathcal{U}(\mathbf{x}^*)$, $\mathbf{b}_{\mathcal{G}}(\mathbf{x}) = \mathbf{b}_{\mathcal{G}}(\mathbf{x}^*)$ implies $\mathbf{b}_{\mathcal{K}}(\mathbf{x}) = \mathbf{b}_{\mathcal{K}}(\mathbf{x}^*)$, and viceversa [3]. Thus the shape error (8) asymptotically converges to zero as long as the bearing error (10) asymptotically converges to zero. This concludes the proof in the light of Prop. III.1. □

Denoting with $\mathcal{N}_i$ the set of neighbors of any i-th agent, $i \in \{1 \dots n\}$, the control law (11) can be rewritten in terms of agent commands as follows revealing its distributed nature

$$\begin{cases} \boldsymbol{\delta}_{p,i} = -k_c \sum\limits_{j \in \mathcal{N}_i} \check{d}_{ij}\mathbf{S}_{p,i}{}^{\top}\mathbf{P}^{\top}(\mathbf{b}_{ij})\mathbf{b}_{ij}^* \\ \qquad\qquad + k_c \sum\limits_{j:i \in \mathcal{N}_j} \check{d}_{ij}\mathbf{S}_{p,i}{}^{\top}\mathbf{R}_i^{\top}\mathbf{R}_j\mathbf{P}^{\top}(\mathbf{b}_{ji})\mathbf{b}_{ji}^*, \\ \boldsymbol{\delta}_{o,i} = k_c \sum\limits_{j \in \mathcal{N}_i} \mathbf{S}_{o,i}{}^{\top}[\mathbf{b}_{ij}]_{\times}^{\top}\mathbf{b}_{ij}^*. \end{cases} \tag{16}$$

According to (16), each agent computes its commands exploiting the recorded bearing measurements ($\mathcal{N}_i$) and those gathered from the agents it is sensed by ($j : i \in \mathcal{N}_j$)[1].

[1]Since the interaction graph is assumed to be directed, the commands computation has to be preceded with the measurement communication.

IV. Numerical Results

In this section, the outlined stabilization control law is compared with a hierarchical combination of existing rigidity based controllers designed for homogeneous formations: the intent is both to show the effectiveness of the proposed solution and to highlight its intrinsic structural simplicity.

A. Preliminary Comparative Assessment

The attention is focused on a heterogeneous formation composed of three fully-actuated UAVs and four fully-actuated UGVs. As per Prob. III.1, the control goal consists in the stabilization of the given formation toward a desired shape: at the beginning all the agents are randomly placed on the (x, y)-plane of $\mathcal{F}_W$; whereas, in the final desired shape the UGVs are required to be located on the corners of a square, while the UAVs fly over them in a triangular configuration with a specific alignment between the two planar shapes, as shown in Fig. 2a.

The performance of the controller (16) is evaluated w.r.t. an ad-hoc strategy that hierarchically solves Prob. III.1 by focusing on the two homogeneous sub-formations composed of only UAVs and only UGVs. Such a strategy envisages to control them in a separate and parallel way and to simultaneously act adjusting the relative displacement $\bar{\mathbf{p}} \in \mathbb{R}^3$ between the centers of mass, the relative orientation $\bar{\mathbf{q}} \in \mathbb{S}^3$ between the local frames of a generic couple made of a UGV and a UAV, and the whole formation scale factor $\rho \in \mathbb{R}_+$. More specifically, the rigidity based distributed controllers proposed in [4], [8] are employed to steer the two sub-formations so that their components achieve the desired poses. In doing this, the aerial and ground sub-formations are modeled as (homogeneous) frameworks $(\mathcal{G}_{\mathrm{A}}, \mathbf{x}_{\mathrm{A}})$ embedded in $SE(3)^3$ and $(\mathcal{G}_{\mathrm{G}}, \mathbf{x}_{\mathrm{G}})$ embedded in $SE(2)^4$, respectively. It is possible to verify that both $(\mathcal{G}_{\mathrm{A}}, \mathbf{x}_{\mathrm{A}})$ and $(\mathcal{G}_{\mathrm{G}}, \mathbf{x}_{\mathrm{G}})$ are IBR according to the general definition given in [3]. Concurrently to the sub-formations stabilization, a leader-follower inspired strategy is employed to adjust the parameters of the whole formation. In practice, the multi-UGVs system acts as leader defining the desired values of $\bar{\mathbf{p}}$, $\bar{\mathbf{q}}$, ρ, and, consequently, the (follower) multi-UAVs system performs the necessary shape-invariant movements, consisting in the translation, the coordinated rotation (namely, rotations of all the agents jointly with the equal rotation of the entire group) and the uniform scaling of the whole sub-formation in $\mathcal{F}_W$. Hereafter, the described control strategy is referred as *multi-action* (MA) controller, while the stabilization law (16) is indicated as *single-action* (SA) controller.

Fig. 2b reports the trajectories followed by the agents from their initial to final positions (grey and black dots, respectively) thanks to the implementation of the SA controller (16). From Fig. 2c, instead, one can observe that the agents trajectories are more complicated when the MA controller is employed. This is due to the fact that the UAVs are required to simultaneously reach their desired poses and to rearrange w.r.t. the whole desired formation shape. Conversely, the SA controller aims at equally distribute the effort among all the agents (based on the sensing graph $\mathcal{G}$).

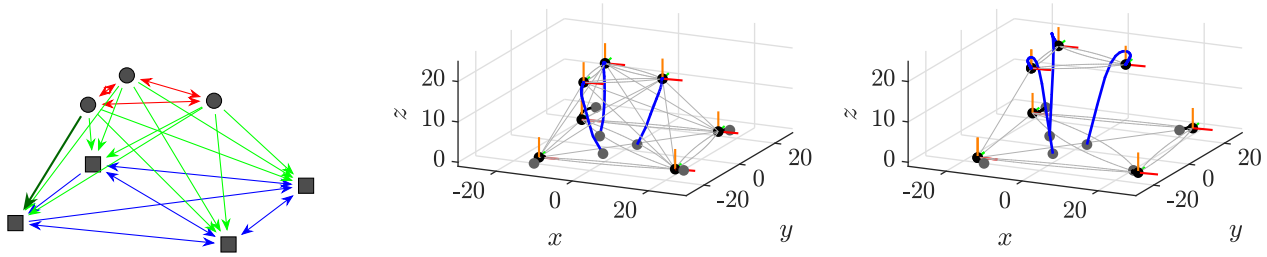

(a) Desired formation shape (b) SA controller (c) MA controller

Fig. 2: heterogeneous formation stabilization. (a) Desired formation shape - UAVs are represented by circles, UGVs by squares; red arrows and blue arrows refer to the edges of $\mathcal{G}_A$ and $\mathcal{G}_G$, respectively, the dark green edge is the one exploited by the leader-follower controller. (b) Performance of the SA controller, (c) performance of the MA controller - the trajectories of the UAVs are depicted in blue, the ones of the UGVs in black.

B. Monte-Carlo Campaign Validation

A Monte-Carlo (MC) simulative campaign has also been conducted accounting for $N = 100$ different realizations of initial conditions of the given formation stabilization problem. To approximate real-world behavior, all bearing measurements have been corrupted with additive Gaussian noise having zero mean and standard deviation $\sigma = 0.5°$. In particular, two different MC tests (with N runs each) have been considered, highlighting the intrinsic trade-off between stabilization speed and control effort.

The first evaluated performance index consists in the *formation settling time* $t_s > 0$, corresponding to the average time required to align the bearing measurements to the given desired ones with a certain tolerance. Formally, t_s is computed as the average time required by the following quantity $\alpha(t) = \frac{1}{m}\sum_{i=1}^{m} \arccos\left(\mathbf{b}_i^\top(\mathbf{x}(t))\mathbf{b}_i^*\right)$ to go below a certain threshold selected as $\bar{\alpha} = 0.75°$. Motivated by the MC approach, the Empirical Cumulative Distribution Function (ECDF) is considered. This is defined as

$$\hat{F}_{t_s}(t) = \frac{1}{N}\sum_{k=1}^{N} \mathbb{1}_{t_s,k}(t), \tag{17}$$

where, for each k-th trial, the indicator function $\mathbb{1}_{t_s,k}(t)$ is equal to one when $t \geq t_s$ and zero otherwise. Conversely, the control effort is investigated through the computation of the ECDF of the input energy required to reach the settling condition. Formally, this is computed as

$$\hat{F}_{E_s}(E) = \frac{1}{N}\sum_{k=1}^{N} \mathbb{1}_{E_s,k}(E), \tag{18}$$

where the indicator function $\mathbb{1}_{E_s,k}(E)$ accounts for the number of trials where $E \geq E_s$ with $E_s = \int_0^{t_s} \|\boldsymbol{\delta}(s)\| ds$.

In the first MC test, the tunable parameters of the SA and MA controllers have been set so that the two solutions turn out to be equivalent in terms of *control effort*. The results are reported on the top of Fig. 3. Observe that the proposed SA controller (blue line) outperforms the MA controller (orange line) as concerns the selling time (left panel). The trend of the ECDF (17) is reported (right panel) also accounting for the stabilization of the aerial and ground sub-formations in the MA scenario (yellow and purple dashed lines). Two observations are in place. First, the UAVs achieve their desired poses ten times faster than the UGVs: this highlights the key role played by the underlying topology. Then, the gap between the ECDF computed in correspondence of the ground multi-agent system stabilization and of the MA controller employment points out that the settling time strongly depends on the alignment between the two sub-formations. In this direction, the slower sub-formation stabilization performance can be interpreted as a lower bound for the settling time in case of MA controller adoption.

The results of the second MC test are reported on the bottom of Fig. 3. In this case, the parameters of the SA and MA controllers are tuned so that the two approaches exhibit the same settling times. In these conditions, the SA approach requires a lower control effort (right panel) implying that the outlined formation controller is more energy-efficient as compared to the MA one but not more effective in terms of settling time (left panel).

The table on the left of Fig. 3 summarizes the main results, specifying the average settling times and the average settling energies for both the MC tests[2], and confirming the overall better performance for the heterogeneous SA controller.

V. Discussion

In this section, the principal aspects of the designed heterogeneous formation control are highlighted. First, note that the proposed distributed approach (16) depends on relative bearing information but also also on the inter-agent distances and relative orientations. Nonetheless, these last can be estimated through distributed consensus algorithms without employing additional sensors [10].

Then, contrarily to most of the existing formation stabilization schemes, the designed control law (11) is not a classical gradient descent procedure, distinguishing w.r.t. the standard bearing based rigid formation controllers [4], [8], [9]. However, taking into account (15), one can observe

[2]These results are given only in terms of average because the wide range of MC realizations yields high values of variance over the whole spectrum of simulations.

		SA	MA
same ctrl effort	t_s	22.1s	32.6s
	E_s	1220	1212
same setl time	t_s	30.9s	31.5s
	E_s	829	1447

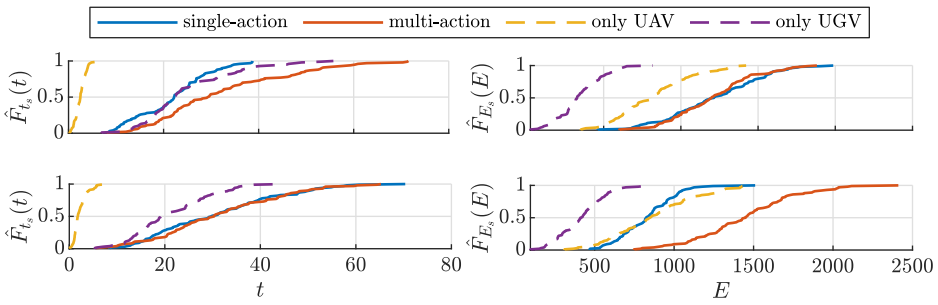

Fig. 3: results of MC tests - the table reports the average value of settling time and required energy, the figures shown the trend of the ECDFs (17) (left) and (18) (right) in correspondence to the fisrt (top) and second (bottom) MC test.

that the proposed controller can be interpreted as a gradient descent solution followed by a re-projection operation necessary to guarantee that the configuration derived from the application of (11) is in $\mathbb{R}^{3n} \times \mathbb{S}^{3^n}$. Such a re-projection is mainly due to the adopted rotation representation.

Finally, the proposed controller presents a single parameter to tune, having a simple structure if compared with the hierarchical MA approach introduced in Sec. IV. This, indeed, results to be structurally more complex involving multiple controllers operating at different levels (each of them, then, involves one or more parameters to tune) and more demanding in terms of agents interactions (sub-formations are required to communicate in a bilateral manner).

VI. Conclusion and Future Works

In this work, bearing rigidity theory is applied to heterogeneous multi-agent systems, confirming to be a powerful tool to address the formation problem. In particular, the bearing rigidity properties of heterogeneous systems emerge from the agents state and measurement domains and from the constraints imposed by the feasibility of their actuation. These elements can be combined into specific selection maps that allow a generalized and unifying approach to the design of stabilization controllers. Numerical simulations are presented and discussed to assess the theoretical findings.

The research avenues that can stem from this work are many and regard both theoretical developments and application scenarios, among which it is worthwhile to mention the exploration of dynamically redundant rigidity schemes for heterogeneous formations, the persistence of formations with directed measurements, split and rejoin strategies for application oriented hierarchical formation control.

Appendix

Observe that the commands computation (16) requires that i-th agent is aware about the relative orientation $\mathbf{q}_{ji}$ w.r.t. the j-th agent able to sense it. Such a quantity can be determined, assuming that a generic pair of agents in the the group are able to measure their relative distance and that the whole formation is IBR. Hereafter, a *rigidity based state estimation procedure* is described: its solution corresponds to the real configuration, in terms of shape, up to a translation and/or coordinated rotation of the whole multi-agent system.

Let denote by $\hat{\mathbf{x}} \in \mathbb{R}^{3n} \times \mathbb{S}^{3^n}$ the state estimate driven by

$$\dot{\hat{\mathbf{x}}} = \mathbf{D}(\hat{\mathbf{q}})\mathbf{S}(\boldsymbol{\delta}_L + \boldsymbol{\delta}) + \mathbf{u}_s, \tag{19}$$

where the vector $\hat{\mathbf{q}} \in \mathbb{S}^{3^n}$ stack the estimation of the agent orientation performed extending the approach presented in [9], the matrices $\mathbf{D}(\cdot)$ and $\mathbf{S}$ play the same role as in (7) and $\boldsymbol{\delta}_L \in \mathbb{R}^c$ is the bearing-based estimator input. In detail, this is selected as

$$\boldsymbol{\delta}_L = k_e \mathbf{B}_{\mathcal{G}}^{\top}(\hat{\mathbf{x}})\mathbf{b}_{\mathcal{G}}(\mathbf{x}) \tag{20}$$

so that, in *static* conditions, the the estimated configuration $\hat{\mathbf{x}}$ converges to the real one. To take into account time-varying configurations, in (19) the feedforward term $\boldsymbol{\delta} \in \mathbb{R}^c$ is added to the scale-matching component $\mathbf{u}_s \in \mathbb{R}^{7n}$. This latter ensures that the scale of the estimated formation approximates the real one. In this direction, a possible solution relies on the exploitation of the measured inter-agent distance and apply a simple proportional controller.

References

[1] H.-S. Ahn, *Formation Control: Approaches to Distributed Agents*. Springer International Publishing, 2020.

[2] S. Zhao and D. Zelazo, "Bearing rigidity theory and its applications for control and estimation of network systems: Life beyond distance rigidity," *IEEE Control Systems Mag.*, vol. 39, no. 2, pp. 66–83, 2019.

[3] G. Michieletto, A. Cenedese, and D. Zelazo, "A unified dissertation on bearing rigidity theory," *IEEE Trans. on Control of Network Systems*, 2021.

[4] G. Michieletto and A. Cenedese, "Formation control for fully actuated systems: a quaternion-based bearing rigidity approach," in *2019 IEEE European Control Conf. (ECC)*, 2019, pp. 107–112.

[5] F. Schiano and P. R. Giordano, "Bearing rigidity maintenance for formations of quadrotor uavs," in *2017 IEEE Int. Conf. on Robotics and Automation (ICRA)*, 2017, pp. 1467–1474.

[6] L. Chen, M. Cao, and C. Li, "Bearing rigidity and formation stabilization for multiple rigid bodies in SE(3)," *Numerical Algebra, Control & Optimization*, vol. 9, no. 3, p. 257, 2019.

[7] G. Stacey and R. Mahony, "The role of symmetry in rigidity analysis: A tool for network localization and formation control," *IEEE Trans. on Automatic Control*, vol. 63, no. 5, pp. 1313–1328, 2017.

[8] D. Zelazo, P. R. Giordano, and A. Franchi, "Bearing-only formation control using an SE (2) rigidity theory," in *IEEE Conf. on Decision and Control (CDC)*, 2015, pp. 6121–6126.

[9] F. Schiano, A. Franchi, D. Zelazo, and P. R. Giordano, "A rigidity-based decentralized bearing formation controller for groups of quadrotor UAVs," in *IEEE/RSJ Int. Conf. on Intelligent Robots and Systems (IROS)*, 2016, pp. 5099–5106.

[10] S. S. Kia, B. Van Scoy, J. Cortes, R. A. Freeman, K. M. Lynch, and S. Martinez, "Tutorial on dynamic average consensus: The problem, its applications, and the algorithms," *IEEE Control Systems Mag.*, vol. 39, no. 3, pp. 40–72, 2019.